

Energy resolved soft X-ray imaging in the Large Helical Device

C. Suzuki, K. Ida, T. Kobuchi, M. Yoshinuma, LHD Experimental Group

National Institute for Fusion Science, 322-6 Oroshi-cho, Toki 509-5292, Japan

Introduction

Soft X-ray imaging technique using a CCD (Charge Coupled Device) camera has recently been applied to the diagnostics of magnetically confined high temperature plasmas [1, 2]. The photon energy range detected by the CCD can be controlled by changing the thickness of a metallic filter inserted in front of the detector for energy resolved measurements. However, it is often difficult to quickly exchange the filters during a single discharge since the durations of most magnetically confined plasmas are typically below several seconds.

In the Large Helical Device (LHD) experiments, long pulse discharges under quasi steady state whose electron density and temperature are of the order of 10^{19} m^{-3} and 1 keV, respectively, can be routinely sustained for several minutes [3]. The energy resolved soft X-ray imaging by a CCD camera may be realized in such long pulse discharges by changing the filter thickness during one shot. In this study we have demonstrated the diagnostic system for such measurements. We report mainly on the diagnostic aspects and the preliminary results in this article, and the detailed physical issues will be reported elsewhere in the future.

Experimental details

The diagnostic system consists of a soft X-ray CCD camera (Andor Technology, DO435-BV) together with a pinhole, a pneumatic mechanical shutter, and a remotely rotatable filter disk which mounts 8 beryllium (Be) filters (99.8% purity) at 45° intervals. The selectable filter thicknesses are 50, 70, 100, 150, 250, 450, 850 and 1650 μm , including a common 50 μm Be window. The diameter of the pinhole can also be chosen out of 0.05, 0.1, 0.2 and 0.4 mm. The CCD camera has been installed in a tangential viewport of the LHD to observe tangential soft X-ray images of the plasmas.

The timing chart of the mea-

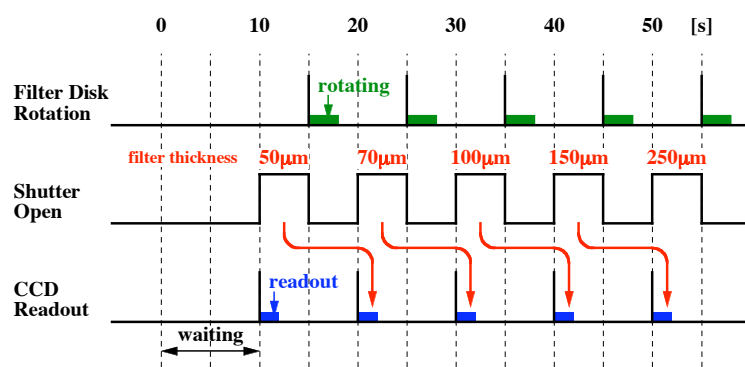


Figure 1: Timing chart of the filter disk rotation, the shutter open, and the CCD readout.

surement is shown in Fig. 1. Since it takes 3–4 seconds to rotate the disk to the adjacent filter in the present system, the frame period and the exposure time of the CCD were adjusted to 10 and 5 seconds, respectively. The measurement begins with opening the shutter and readout the initial dark charge of the CCD after waiting initial 10 seconds of the discharge until the plasma reaches a quasi steady state. The shutter is closed after 5 seconds exposure, and the rotation of the filter disk is simultaneously triggered to move to the next filter. Therefore the CCD is never exposed to the plasma emission during the rotation of the filter disk. After the rotation of the filter is finished, the next frame begins with opening the shutter again, during which the readout of the previous frame can be carried out at once because the frame transfer type CCD is used.

An image for a specific photon energy range can be obtained by taking the difference between two signals measured with different filter thicknesses. Figure 2 shows overall detection efficiency curves for the 7 different combinations of the adjacent Be filter thicknesses used in this study. The effects of the CCD quantum efficiency and the impurities in the filter material are taken into account in Fig. 2. Typical photon energies observed for each difference correspond to the energies at the peaks of these curves, which range from 1.9 to 4.8 keV.

Preliminary results and analyses

Figure 3 illustrates contours of the two dimensional images obtained from the signal differences (a) between 70 and 100 μm filter thicknesses, and (b) between 450 and 850 μm , which were measured in a long-pulse discharge sustained by ion cyclotron resonance heating (ICRH). The central electron temperature measured by a Thomson scattering diagnostic was about 1.3 keV at 8.9 s from the beginning of the discharge. The diameter of the pinhole was set at 0.1 mm. The hardware binning of 2×2 CCD pixels results in 512×512 superpixels in major radius (R) and vertical (Z) directions. In addition, 4×4 superpixels are averaged when the contours are drawn.

It is apparently shown that the profile of Fig.3 (a) is rather broader than that of Fig.3 (b). According to Fig. 2, photon energies

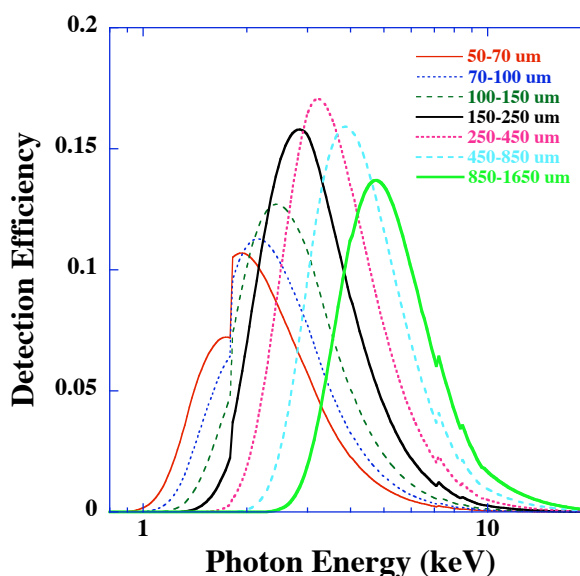


Figure 2: Detection efficiency curves for the differences between adjacent Be filter thicknesses used in this study, including the CCD quantum efficiency.

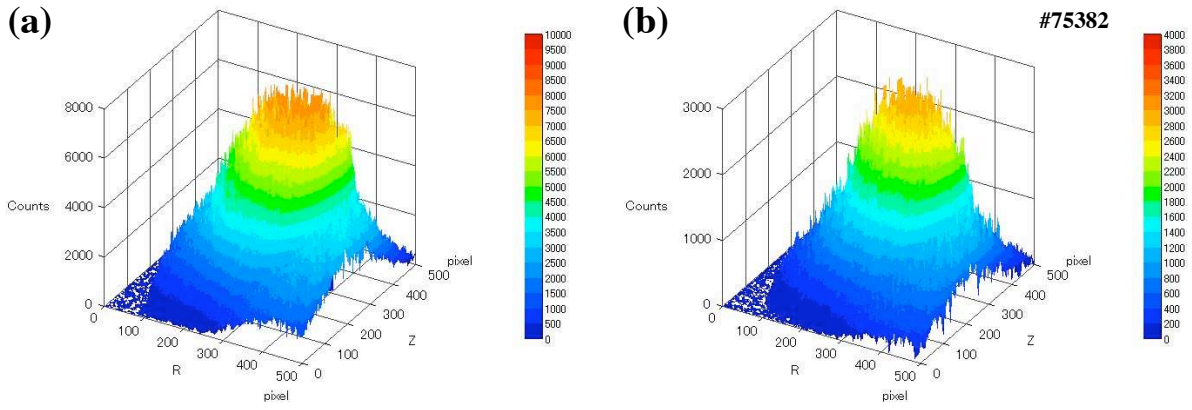


Figure 3: Contours of the two dimensional images obtained from the signal differences (a) between 70 and 100 μm filter thicknesses, and (b) between 450 and 850 μm .

which mainly contribute to the signals are around 2.2 and 3.9 keV for (a) and (b), respectively. Therefore the observed difference in the profile is basically reasonable since the profile of 3.9 keV photons tends to be more peaked than that of 2.2 keV ones.

Since power spectra of continuum radiations (bremsstrahlung and bound-free transitions) have dependence on photon energy (E) expressed by a factor $E \exp(-E/T_e)$, where T_e is electron temperature, the dependence of signal intensity on filter combination for a given T_e can be calculated by integrating the product of a power spectrum and a detection efficiency curve shown in Fig. 2. As an initial step of the analyses, we have compared the dependences of the measured signal intensities on filter combinations with that of the calculated ones. The 7 images for the differences between the adjacent filters measured in the same discharge as Fig. 3 are divided into 16×16 zones by averaging in 32×32 superpixels. Figure 4 shows the measured intensity in a zone near the center chord plotted against the photon energy at the maximum efficiency for each filter combination. The circle

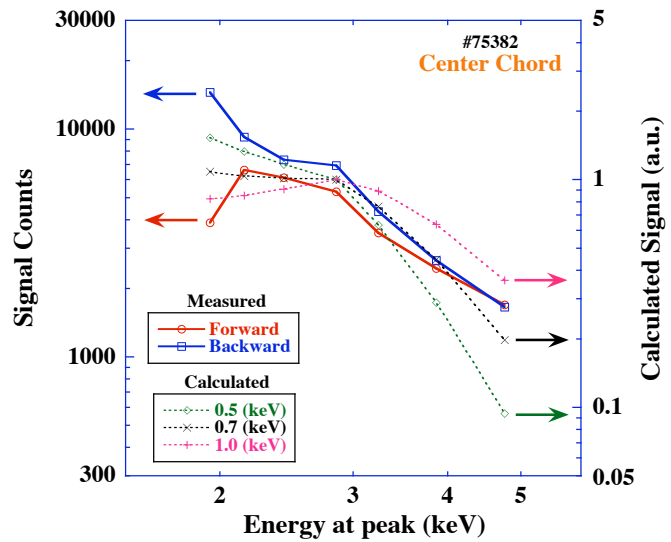


Figure 4: Signal intensity near the center chord plotted against the photon energy at the maximum efficiency for each filter combination. The calculated intensities for the electron temperatures of 0.5, 0.7 and 1.0 keV are also plotted.

and square symbols denote the data obtained by the forward and backward rotations of the filter disk, respectively, in the same shot. Therefore the disagreement between the forward and backward is due to the slow change in the emission during the discharge. Among the calculated intensities for various electron temperatures, the most similar one to the data of the center chord is the one for 0.7 keV as plotted by times symbols in Fig. 4.

According to Fig. 4, the effective (line-integrated) electron temperature for the center chord seems to be roughly 0.7 keV. However, the effects of line radiations should be discussed especially in higher energy range since the spectrum of a pulse height analyzer (PHA) [4] obtained in a similar ICRF discharge indicates that the line spectra from iron, nickel and titanium K_{α} lines could not be negligible.

Summary and future plans

We have developed a diagnostic system for energy resolved soft X-ray imaging in a long pulse LHD discharge by using a CCD camera and Be filters with different thicknesses. As a result, two dimensional images for different photon energy ranges have successfully been measured by taking differences between two signals with adjacent filter thicknesses, and the clear difference in the profile has been observed between them. The dependence of the measured signal intensities on the filter combination was compared with the calculation for the continuum radiation of given electron temperatures, which results in the rough estimation of the effective electron temperature. For the check of the effect of impurity line emission without the PHA, we will develop another soft X-ray CCD system mainly used for photon counting mode in the near future. In addition, the measurement in a long pulse discharge by electron cyclotron resonance heating (ECRH) will be planned because the effect of impurity line emission would be weaker.

Acknowledgments

This work is partly supported by a grant-in-aid for scientific research from MEXT. This work is carried out under budget code NIFS06ULBB510.

References

- [1] Y. Liang *et al.*, Plasma Phys. Control. Fusion **44**, 1383 (2002)
- [2] T. Kobuchi *et al.*, Plasma Phys. Control. Fusion **48**, 789 (2006)
- [3] R. Kumazawa *et al.*, Nucl. Fusion, **46**, S13 (2006)
- [4] S. Muto, S. Morita, and LHD Experimental Group, Rev. Sci. Instrum. **72**, 1206 (2001)